Modeling the Coupled Difference Threshold of Perceiving Mass and Stiffness from Force

Fu, Wei; van Paassen, Rene; Mulder, Max

DOI
10.1109/SMC.2018.00???

Publication date
2018

Document Version
Accepted author manuscript

Published in
Proceedings of the IEEE International Conference on Systems, Man, and Cybernetics

Citation (APA)
Fu, W., van Paassen, R., & Mulder, M. (2018). Modeling the Coupled Difference Threshold of Perceiving Mass and Stiffness from Force. In L. O'Conner (Ed.), *Proceedings of the IEEE International Conference on Systems, Man, and Cybernetics: Myazaki, Japan, 2018* (pp. 1427 - 1432). IEEE. https://doi.org/10.1109/SMC.2018.00???

Important note
To cite this publication, please use the final published version (if applicable).
Please check the document version above.

Modeling the Coupled Difference Threshold of Perceiving Mass and Stiffness from Force

Wei Fu, M. M. (René) van Paassen, Max Mulder
Faculty of Aerospace Engineering
Delft University of Technology
Delft, the Netherlands 2629 HS
Email: {W.Fu-1; M.M.vanPaassen; M.Mulder}@tudelft.nl

***Abstract*—Just notable difference (JND) thresholds for the perception of manipulator dynamic properties are relevant for tele-operation and simulation of vehicles. Manipulator dynamic properties are characterized by multiple variables (describing mass, spring and damping for a linear manipulator) and the JND threshold for any of these variables is affected by variation in the remaining variables. In previous work, we demonstrated and modeled the coupling of the stiffness JND and the mass JND, and investigated the effects of stiffness and mass properties on the damping JND. In this work we investigate how changes in the damping parameter affect the JND in perceiving stiffness and mass. In an experiment our subjects were instructed to discriminate between different levels of manipulator's stiffness or mass, while tracking a prescribed sinusoidal manipulator movement. Results show that the JND in spring force and the JND in inertia force are identical, and increase for higher damping levels. The JND model developed in our previous work can successfully describe the experimental observations, thereby providing an extension of Weber's law. The impedance of the manipulator is considered as the reference stimulus in the frequency domain, so that a single ratio describes the JND thresholds for all three properties.**

***Index Terms*—Just noticeable difference, Mass-spring-damper systems, Frequency response function, Weber's law, haptics**

I. Introduction

In manual control tasks, a control manipulator serves as the haptic interface between human and machine. The operator can perceive force feedback while moving the manipulator to interact with the dynamic system. Through observing the relation between the applied manipulator movement and the perceived force feedback, human operators can estimate the mechanical properties – mass, stiffness and damping – of the *total* dynamic system, i.e., manipulator and environment.

For manual control tasks, rendering the proper dynamic information is important for a haptic interface to help the human operator form an internal model on which skills and proficiency rely [1], [2]. Moreover, an accurate simulation of the desired impedance is also crucial for the therapeutic exercise carried out for rehabilitation [3]. However, due to the limitations of soft/hardware and possible distortion by data transmission, the information that the force feedback conveys about the mechanical properties – the inertia, spring and damping force components – is inevitably distorted. This problem is particularly pronounced in cases where the interaction is remote, as in bilateral tele-operations [4], [5].

It is therefore important to know how large a distortion of the force must be to cause different human perception of mechanical properties. This knowledge can help designers to better tune the settings of their haptic interfaces, depending on the task requirements. That is, a task that requires operators to very accurately distinguish between different mechanical properties of the dynamic environment they interact with will require different settings than a task which does not.

Human just noticeable differences (JND) in mass, stiffness and damping properties have been investigated during the last few decades [6], [7], [8], [9], [10]. From this it appears that Weber's law, which states that the JND is proportional to the reference stimulus, applies when each of the three properties is rendered to humans *in isolation*.

The dynamics conveyed by the manipulator are usually defined by more than one mechanical property alone, however, and the effects of manipulating one parameter on the JND of *another* parameter have been largely overlooked. When a mass-spring-damper system is rendered to humans, the JND in perceiving the damping force violates Weber's law as the stiffness and mass properties vary [11], [12]. In our latest work, we discovered that when modeling the JND in the frequency domain, using the frequency response function (FRF) between force feedback and manipulator deflection, all these relations could be explained and understood [12], [13]. For instance, we found that the frequency response magnitude of the damping JND was proportional to the frequency response magnitude of the *combined* mass-spring-damper system. We also found that the JNDs in perceiving stiffness and mass were *coupled* [12], [13].

The present study continues on our previous work [12], [13], of which the findings will be discussed in greater detail in Section II. The objective of this paper is to further explore the relations among these three mechanical properties, and in particular study the effects of changing the damping parameter on the joint JND in perceiving spring and inertia forces.

The contributions of this paper are summarized as follows:

1) From an experiment with human participants, we find that the JNDs in spring and inertia forces are identical and independent of the excitation frequency. We also find that the JNDs violate Weber's law when the damping property varies: They become higher as the damping increases.

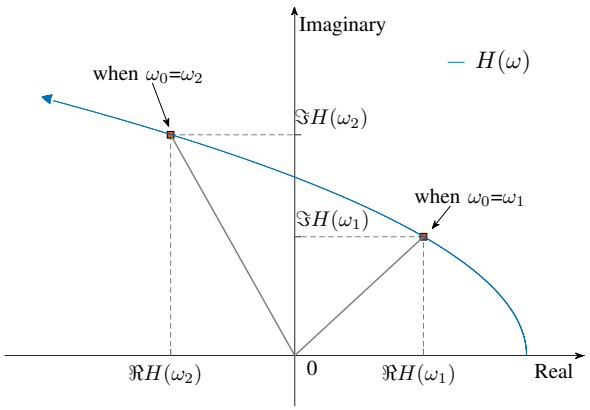

Fig. 1. The Nyquist plot of $H(\omega)$ with typical settings of k, m and b coefficients. The arrow of the curve indicates the increase of frequency. The frequency responses at two frequencies (ω_1 and ω_2) are marked as examples.

2) A frequency-domain model is used to describe the *joint* JND in the perception of stiffness and mass. We show that the frequency response magnitude of this joint JND is proportional to the frequency response magnitude of the combined mass-spring-damper system.

The remainder of this paper is organized as follows: In the following section, we will further discuss our damping JND model and the joint JND in stiffness and mass. In Section III we design an experiment to investigate human JND in perceiving stiffness and mass from force. In Section IV we analyze the results of the experiment and formulate the model for the JND. Section V discusses our work and practical applications. Section VI concludes our contributions.

II. Overview of Previous Work

Assume that the dynamics rendered by a haptic interface (a control manipulator) are represented by a mass-spring-damper system. The open-loop dynamics from the manipulator deflection angle to the force feedback, can then be expressed with the frequency response function (FRF):

$$H(\omega) = \frac{T(\omega)}{\Theta(\omega)} = \underbrace{k - m\cdot\omega^2}_{\Re H(\omega)} + \underbrace{b\cdot\omega}_{\Im H(\omega)}\cdot j \tag{1}$$

Here $\Theta(\omega)$ and $T(\omega)$ denote the Fourier transforms of the deflection angle $\theta(t)$ and the torque feedback $\tau(t)$, respectively. $\Re H(\omega)$ and $\Im H(\omega)\cdot j$ denote the real and imaginary parts of the complex-valued FRF. Without loss of generality, in the remainder of this section we refer to torque as force.

For any given excitation movement, a change in the harmonic force response of the system results from a change in the FRF. Therefore modeling *the JND in perceiving mechanical properties from force* is equivalent to modeling *the JND in the FRF*. Fig. 1 shows a plot of $H(\omega)$ with typical settings of k, m and b. The JND in the FRF specifies a region within which a change in the curve does not lead to a change in the operator's perception of the system's force response.

Each point of the curve determines the system's response at a particular frequency. The characterization of the JND can be simplified by investigating individual frequencies. Now consider that the system is only excited at a particular frequency ω_0, i.e., the excitation movement is a sinusoidal signal with frequency ω_0. The force response of the system ($T(\omega)$) is then also a sinusoidal signal with the same frequency, but with a different amplitude and phase which are determined by $H(\omega_0)$. According to Eq. (1), $T(\omega)$ can be divided into two components: the responses of the real and imaginary parts.

As can be seen from Eq. (1), the real part $\Re H(\omega_0)$ is a *combined* frequency response of stiffness and mass properties. It acts as a gain which generates a force response that is either in phase with (if $\Re H(\omega_0) > 0$), or exactly opposing (if $\Re H(\omega_0) < 0$), the sinusoidal position input. We found that humans *cannot isolate* the information about either of the stiffness and mass properties from this combined force [12], [13], [14]. That is, this combined force is perceived as a *spring force* when $\Re H(\omega_0)$ is *positive* (e.g., $\omega_0 = \omega_1$ in Fig. 1), and it is perceived as an *inertia force* when $\Re H(\omega_0)$ is *negative* (e.g., $\omega_0 = \omega_2$) [1]. One can imagine that the changes in m and k, which result in a particular change in this combined force – and with that, a particular change in the perception – are not unique. This suggests that the JNDs in the perception of these two mechanical properties are coupled in the same way as their responses:

$$\Delta\Re H(\omega) = \Delta k_{jnd} - \Delta m_{jnd}\cdot\omega^2 \tag{2}$$

Here, Δk_{jnd} and Δm_{jnd} denote the stiffness JND and mass JND, respectively. We use $\Delta\Re H(\omega)$ to represent their combined response: the JND in the real part $\Re H(\omega)$.

Now, the imaginary part $\Im H(\omega_0)\cdot j$ is the frequency response of the damping property. Due to the imaginary unit j, this part generates a *damping force* which is 90 degrees out of phase with the manipulator movement: a force proportional to the *velocity*. Humans are able to distinguish the damping force from the combined force response of stiffness and mass [12]. Because of this, the JND in perceiving the damping should be distinguished from that of the stiffness and mass. Here we express the JND in the perception of the damping force with the JND in $\Im H(\omega)$:

$$\Delta\Im H(\omega) = \Delta b_{jnd}\cdot\omega \tag{3}$$

Our current interest lies in the two JNDs in Eqs. (2) and (3) at each frequency. Although these two JNDs relate to different mechanical properties, the interaction between the real and imaginary parts must be taken into account. It has been demonstrated that $\Delta\Im H(\omega)$ is affected by $\Re H(\omega)$ (this means that the damping JND is affected by the stiffness and mass properties) [11], [12]. This effect was studied for ω = 6 [rad/s] in our previous work [12], [13], in which a model was obtained to express $\Delta\Im H(\omega)$ as:

$$\left|\frac{\Delta\Im H(\omega)}{H(\omega)}\right| = c\,, \tag{4}$$

[1]Here spring force refers to the force that is proportional to the position (manipulator displacement). Inertia force refers to the force that is proportional to acceleration (this force becomes maximum where the direction of the manipulator movement changes.)

Here c is a constant. The effect of $\Re H(\omega)$ is implicitly shown by this model. The magnitude of $H(\omega)$ increases when the real part $\Re H(\omega)$ increases, as a result the damping JND becomes higher.

Eq. (4) can be seen as an extension of Weber's law. This model indicates that the frequency response magnitude of the damping JND is a constant fraction of the frequency response magnitude of the combined system. In other words, this equation expresses the proportional relation between the system's FRF and the JND in its imaginary part. This demonstrates an effect of the real part on the JND in the imaginary part. The effect of the imaginary part on the real part has yet to be revealed, but is expected to be similar because the two variables are orthogonal. In other words, we assume that the JND in the perception of the stiffness and mass becomes higher when the damping increases.

In order to verify this, $\Delta\Re H(\omega)$ needs to be measured for different damping levels. Due to the fact that the spring force and the inertia force have opposite directions, the human JND in the perception of these two forces may be different. Therefore, the investigation of $\Delta\Re H(\omega)$ should be considered for two different cases, i.e., *the JND in the spring force* ($\Delta\Re H(\omega)$ in the case of positive $\Re H(\omega)$) and *the JND in the inertia force* ($\Delta\Re H(\omega)$ in the case of negative $\Re H(\omega)$).

The objective of this study is to test the validity of the model in Eq. (4) for the JND in the real part. The dependence of this model on the excitation frequency will also be investigated. In the following section, we discuss an experiment designed to study both cases.

III. Experiment Design

A. Conditions

The objectives of the experiment are threefold; we want to establish the effect of changes in the manipulator damping coefficient on the perception of spring (1) and on the perception of inertia (2) forces. In addition, we want to explore the effect of the frequency with which the manipulator is deflected on the thresholds (3). Since the procedure to determine a single threshold value is fairly long, we limited the number of conditions by not creating a full factorial experiment.

The experiment to measure $\Delta\Re H(\omega)$ (the JND in the real part) has nine different conditions, expressed in terms of the real and imaginary part of the FRF. Details of conditions are given in Table I. We label the conditions as Ci for an easy reference in the following content.

The JND measurement for each condition will be collected at a single frequency of excitation ω_i. This is achieved by asking subjects to apply (an approximately) sinusoidal movement to the manipulator during the experiment. More details about this prescribed manipulator movement will be given in Section III-D.

Conditions C1-5 define a positive $\Re H(\omega_i)$, corresponding to a spring force, and five different ratios of $\Im H(\omega_i)$ to $\Re H(\omega_i)$ ranging from 0 to 2. The measurements for these five conditions will demonstrate how different levels of damping affect $\Delta\Re H(\omega_i)$. Conditions C6-7 are designed with a different excitation frequency ω_i to investigate the effect of the frequency on the JND. A negative $\Re H(\omega_i)$, corresponding to an inertia force, and two different ratios are defined in C8-9 to study the effect of force direction (the sign of $\Re H(\omega_i)$) on the JND. Fig. 2 shows the settings of the nine conditions on the complex plane.

TABLE I
Conditions of the Experiment

Condition	$\Re H(\omega_i)$	$\Im H(\omega_i)$	ω_i ([rad/s])	$r=\left\lvert\frac{\Im H(\omega_i)}{\Re H(\omega_i)}\right\rvert$
C1	1.26	0.0	6	0.0
C2	1.26	0.63	6	0.5
C3	1.26	1.26	6	1.0
C4	1.26	1.89	6	1.5
C5	1.26	2.52	6	2.0
C6	1.26	0.0	8	0.0
C7	1.26	2.52	8	2.0
C8	-1.26	0.0	6	0.0
C9	-1.26	2.52	6	2.0

Note that all the variables in this paper are defined using the rotational convention.

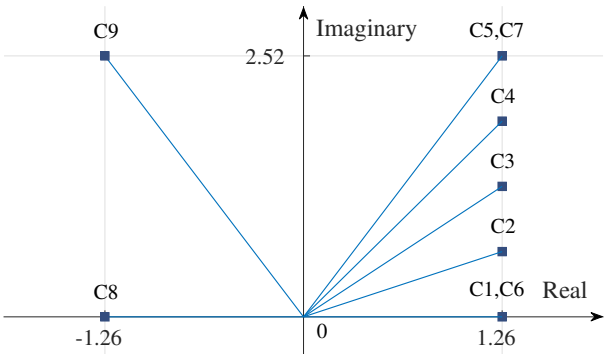

Fig. 2. Conditions of the experiment shown on the complex plane.

In order to obtain the desired settings of $\Re H(\omega_i)$ and $\Im H(\omega_i)$ in Table I, the three coefficients k, m and b in Eq. (1) were set in the following way[2]:

$$k = \begin{cases} \Re H(\omega_i) + 0.01{\omega_i}^2 & \text{, if } \Re H(\omega_i) > 0 \\ 0 & \text{, if } \Re H(\omega_i) < 0 \end{cases}$$
$$m = \begin{cases} 0.01 & \text{, if } \Re H(\omega_i) > 0 \\ \dfrac{-\Re H(\omega_i)}{\omega_i^2} & \text{, if } \Re H(\omega_i) < 0 \end{cases} \quad (5)$$
$$b = \frac{\Im H(\omega_i)}{\omega_i}$$

As can be seen from Eq. (1), at a single frequency the combination of k and m that yields a particular $\Re H(\omega_i)$ is not unique. By using the settings specified in Eq. (5), $\Delta\Re H(\omega_i)$

[2]Ideally, the mass for the simulated manipulator m should have been chosen to be zero for $\Re H(\omega_i) > 0$. However, to maintain stability of the simulation, a minimal mass of 0.01 [kg $\cdot$ m^2] is maintained. The stiffness k is therefore adjusted accordingly to obtain the desired value of $\Re H(\omega_i)$.

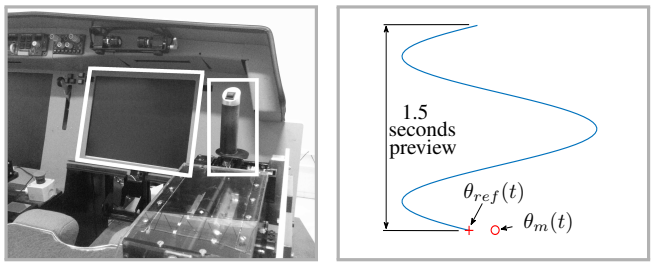

(a) (b)

Fig. 3. (a): The apparatus used in the JND experiment. The side-stick manipulator and the LCD screen are marked by white rectangles. The LCD screen only displays the visual presentation of the tracking task. (b): The tracking task shown on the LCD screen. To reduce the manipulator deflection tracking error exampled in this figure, the subject has to push the manipulator towards the left.

can be simply obtained through measuring the stiffness JND (when $\Re H(\omega_i) > 0$) and the mass JND (when $\Re H(\omega_i) < 0$).

B. Apparatus and participants

The experiments were performed in the Human-Machine Interaction Laboratory at the faculty of Aerospace Engineering, TU Delft. An illustration of the devices is given in Fig. 3a. An admittance-type side-stick manipulator driven by an electro-hydraulic motor was used in the experiment. Details of the manipulator can be found in [12]. The manipulator can move in the left/right direction (lateral). The torque-to-deflection manipulator dynamics specified by Eq. (1) can be accurately rendered to the human operator at the two desired frequencies of excitation. The settings of the mass, spring and damper coefficients (m, k and b in Eq. (1)) of the rendered manipulator dynamics can be configured according to different conditions.

An LCD screen, placed in front of the subject, was used to help subjects follow the prescribed sinusoidal manipulator movement (see Section III-D).

Nine subjects participated ($n = 9$), all right-handed and without a history of impairments in moving their arm or hand. An informed consent form was signed before the experiment.

C. Procedure

In this study, only the upper JNDs were investigated. The JND for each condition was measured by a one-up/two-down staircase procedure [15]. The procedure generally needed approximately 20-30 trials to converge. Each trial consisted of two 6.3-second simulations. In one simulation the manipulator was configured with the reference setting which is the setting of the condition (see Table I and Eq. (5)). In the other simulation the manipulator was configured with the controlled setting which only differed from the reference setting in the tested mechanical property S (stiffness or mass) by an adjusted increment δS. The sequence of the two simulations in each trial was randomly based on a prior probability of 0.5.

In each simulation, the subject was asked to perceive the manipulator dynamics while moving the manipulator with the prescribed sinusoidal deflection. After each trial, the subject was asked to report in which of the two simulations he or she experienced a higher level of manipulator stiffness (conditions C1-7) or manipulator mass (conditions C8-9). δS for the next trial was then adjusted according to the correctness of the subjects' answer. In this way, δS gradually converged to the JND. More details about this staircase procedure can be found in our previous work [12].

TABLE II
JND MEASUREMENTS, SHOWN AS SAMPLE MEANS AND 95% CONFIDENCE INTERVALS CORRECTED FOR BETWEEN-SUBJECT VARIABILITY

$\Delta\Re H(\omega_i)$ (condition)	ratio $r=\left\lvert\frac{\Im H(\omega_i)}{\Re H(\omega_i)}\right\rvert$				
	0.0	0.5	1.0	1.5	2.0
Δk (C1-5)	.15±.07	.15±.05	.22±.05	.27±.06	.34±.05
Δk (C6-7)	.14±.04	-	-	-	.29±.06
$\Delta m \cdot \omega_i^2$ (C8-9)	.16±.05	-	-	-	.30±.08

D. Prescribed manipulator movement

To ensure that our subjects excited the manipulator at the desired excitation frequency, they performed a preview tracking task [16] in each simulation, see Fig. 3b. The reference manipulator deflection is calculated according to:

$$\theta_{ref}(t) = 0.37 \cdot \sin(\omega_i t) \tag{6}$$

Here ω_i denotes the desired frequency of excitation (6 or 8 [rad/s], see Table I). In addition, the first and last cycles of this prescribed movement are used as fade-in and -out phases. The movement amplitude gradually increases from 0 to 0.37 during the fade-in phase, and decreases from 0.37 to 0 during the fade-out phase. To perform the tracking task, the subject needs to reduce the tracking error between the current manipulator deflection $\theta_m(t)$ (shown by "$\circ$" in Fig. 3b) and the current reference deflection $\theta_{ref}(t)$ (shown by "+"). The two symbols only move horizontally. The visual preview, shown as a winding curve (blue line), contains 1.5-second future information of the reference deflection θ_{ref}. It moves downwards as time progresses.

IV. Results and Model Validation

A. Experimental results

All participants were able to adequately perform the tracking task. The actual movement frequencies in all experimental runs were evaluated, and found to only deviate from 6 [rad/s] by less than 0.1 [rad/s]. Therefore the effects of the testing factors at the desired conditions can be accurately reflected by the experimental observations. Table II summarizes the results of the experiment. The results are also shown in Fig. 4 for a clear illustration. When examining the JNDs for conditions C1-5, an obvious increase can be seen as the ratio r increases. A one-way repeated measures ANOVA performed for these five conditions revealed that the effect of r was

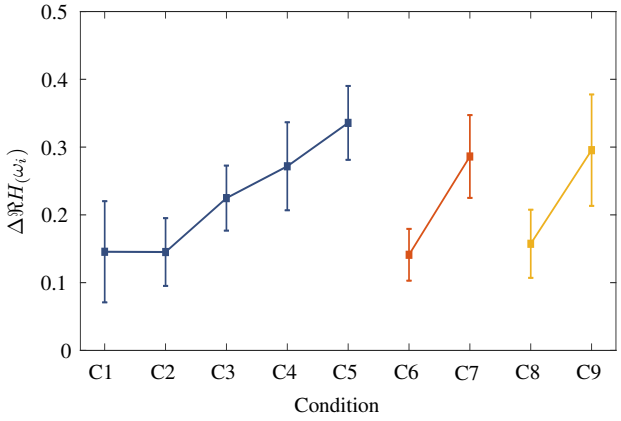

Fig. 4. Measurements of $|\Delta\Re H(\omega_i)|$ shown with the sample means and 95% confidence intervals corrected for between-subject variability.

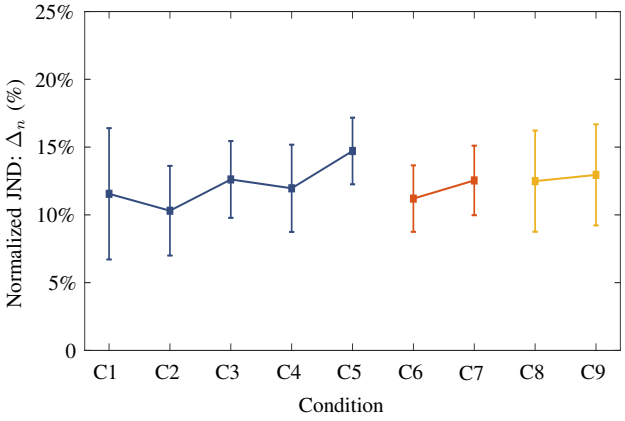

Fig. 5. The $|\Delta\Re H(\omega_i)|$ normalized to the system magnitude $|H(\omega_i)|$. The normalized JNDs are shown with the sample means and 95% confidence intervals corrected for between-subject variability.

significant (F(4,32) = 8.1, $p < .01$). Two separate one-way repeated measures ANOVAs were performed to investigate: (1) the differences among conditions C1,6,8; (2) the differences among conditions C5,7,9. Results showed that when r = 0.0 (conditions C1,6,8) the variations in the excitation frequency ω_i and the sign of $\Re H(\omega_i)$ both failed to cause any significant change in the JNDs (F(2,16) = .21, $p > .05$). The same conclusion was drawn when r = 2.0 (conditions C5,7,9) (F(2,16) = .74, $p > .05$).

The above results confirm that the imaginary part affects the JND in the real part, i.e., $\Im H(\omega)$ affects $\Delta\Re H(\omega)$. This shows that the JNDs in perceiving the stiffness and mass properties from force violate Weber's law when the damping varies. The JNDs and the observed effect of $\Im H(\omega)$ are independent, however, of the *sign* of $\Re H(\omega)$ and the excitation frequency. In other words, humans have similar JNDs in perceiving the spring and inertia forces. The level of the JNDs does not vary with small variations in the frequency of excitation movements. When damping is higher (r increases), changes that can cause different perception in stiffness and mass increase.

B. Model validation

In order to check the validity of a model similar to Eq. (4), the JND measurements shown by Table II are normalized to the corresponding system magnitude according to the following equation:

$$\Delta_n = \left| \frac{\Delta\Re H(\omega_i)}{H(\omega_i)} \right| \tag{7}$$

Fig. 5 shows Δ_n obtained for all the nine conditions. A one-way repeated-measures ANOVA shows no significant differences among the nine conditions (F(8,64) = .59, $p > .05$). This confirms the validity of our model, and indicates that the magnitude of $\Delta\Re H(\omega)$ is proportional to the magnitude of $H(\omega)$.

Thus, an extension of Weber's law for the joint JND in perceiving stiffness and mass from force can be formulated. When regarding the frequency response of a dynamic system as the reference stimulus, the relative change along the real axis of the complex plane is constant:

$$\left| \frac{\Delta\Re H(\omega)}{H(\omega)} \right| = \left| \frac{\Delta k_{jnd} - \Delta m_{jnd} \cdot \omega^2}{k - m \cdot \omega^2 + b \cdot \omega \cdot j} \right| = p \tag{8}$$

Here the ratio p is a constant. We found a representative numerical value (12.2%), by averaging the results shown in Fig. 5 over all the conditions. It is worth mentioning that this value is similar to that of perceiving the damping force (roughly 9% [12]).

V. Discussion

In this study we have demonstrated the effect of the damping on human perception of stiffness and mass properties of a dynamic system. Due to the variation in the damping, Weber's law, which is commonly used to estimate the JNDs in the perception of mechanical properties, can not describe the experimental observations. As expected, the JND in spring and inertia forces increases as the damping increases. This phenomenon is successfully characterized by a model which was previously found to be valid for effects of spring and mass changes on the damping JND.

The experimental results also demonstrate the validity of the model for different excitation frequencies. The normalized JNDs given by the model are approximately identical for the two chosen frequencies. Although the manipulated variation in the excitation frequency is relatively small, this conclusion reliably applies in cases where the excitation movement is mainly generated by the human arm. This scenario covers a wide range of manual control tasks, such as car driving and aircraft flying, in which the main energy of human control input usually lies below 2-3 Hz in the power spectrum.

The effect of the amplitude of the excitation movement was excluded from the investigation. This is because the movement amplitude has no effect on the relative force JND (Weber fraction) [17], provided that the considered amplitude is moderate (not too small or too large).

An extension of Weber's law for the perception of stiffness and mass is obtained using this model (see Eq. (8)). With this extension the performance of a haptic interface, in terms of the rendering of stiffness and mass properties of a dynamic system, can be easily evaluated. The evaluation can be done in the frequency domain by examining the differences between the desired dynamics and the rendered dynamics for the frequency range of considered excitation. A haptic interface can potentially lead the operator to have a different perception, if there exists a frequency where the real-part difference is larger than the corresponding threshold (12% of the frequency response magnitude of the desired dynamics).

Moreover, the findings of this study give a number of insights into the design of haptic interfaces. On the one hand, a higher level of damping allows for larger distortions of the spring and inertia forces. This reduces the requirements on the system performance. The high demands, for simulating mass and high levels of stiffness, on the gain of the control system can be alleviated, which in turn can be beneficial to system stability [18]. On the other hand, the increase of damping also reduces the human ability to perceive a change in stiffness and mass properties. When damping injection [19] is used to guarantee the stability of a haptic interaction, this issue must be taken into account for cases where discriminating between different levels of stiffness or mass is important for the task at hand.

VI. Conclusion

In this study we investigated the human JND in the perception of spring and inertia forces, and the effect of system damping settings on this JND. An experiment employing an adaptive staircase procedure was conducted to measure the stiffness and mass JND under conditions in which different damping levels and excitation frequencies are defined. Results show that subjects have similar JNDs in perceiving spring and inertia forces, and these JNDs are independent of the frequency whith which the manipulator is moved. They become higher, however, to an equal extent, when the damping increases. We successfully characterized the experimental observations using a model obtained in our previous study. We found that the JND in the joint frequency response of stiffness and mass (the real part) is proportional to the frequency response magnitude of the dynamic system.

References

[1] R. C. Miall and D. M. Wolpert, "Forward models for physiological motor control," *Neural Networks*, vol. 9, no. 8, pp. 1265–1279, 1996.

[2] M. M. Van Paassen, J. C. Van Der Vaart, and J. A. Mulder, "Model of the neuromuscular dynamics of the human pilot's arm," *Journal of Aircraft*, vol. 41, no. 6, pp. 1482–1490, 2004.

[3] Y. Tanaka, T. Abe, T. Tsuji, and H. Miyaguchi, "Motion dependence of impedance perception ability in human movements," in *Proceedings of the First International Conference on Complex Medical Engineering*. Citeseer, 2005, pp. 472–477.

[4] B. Hannaford, "Stability and performance tradeoffs in bi-lateral telemanipulation," in *Robotics and Automation, 1989. Proceedings., 1989 IEEE International Conference on*. IEEE, 1989, pp. 1764–1767.

[5] D. A. Lawrence, "Stability and transparency in bilateral teleoperation," *IEEE Trans. Robotics and Automation*, vol. 9, no. 5, pp. 624–637, 1993.

[6] L. A. Jones, "Kinesthetic sensing," in *Human and Machine Haptics*. MIT Press, 2000.

[7] H. Z. Tan, N. I. Durlach, G. L. Beauregard, and M. A. Srinivasan, "Manual discrimination of compliance using active pinch grasp: The roles of force and work cues," *Perception & Psychophysics*, vol. 57, no. 4, pp. 495–510, 1995.

[8] G. L. Beauregard, M. A. Srinivasan, and N. I. Durlach, "The manual resolution of viscosity and mass," in *ASME Dynamic Systems and Control Division*, vol. 1, 1995, pp. 657–662.

[9] W. Fu, M. M. van Paassen, and M. Mulder, "On the relationship between the force JND and the stiffness JND in haptic perception," in *Proc. of the ACM Symp. on Applied Perception*. ACM, 2017, p. 11.

[10] ——, "The influence of discrimination strategy on the JND in human haptic perception of manipulator stiffness," in *AIAA Modeling and Simulation Technologies Conference*, 2017, p. 3668.

[11] E. M. Rank, T. Schauß, A. Peer, S. Hirche, and R. L. Klatzky, "Masking effects for damping JND," in *International Conference on Human Haptic Sensing and Touch Enabled Computer Applications*. Springer, 2012, pp. 145–150.

[12] W. Fu, A. Landman, M. M. van Paassen, and M. Mulder, "Modeling human difference threshold in perceiving mechanical properties from force," *IEEE Trans. Human-Machine Systems*, vol. 48, no. 4, pp. 359–368, Aug 2018.

[13] W. Fu, M. M. van Paassen, O. Stroosma, and M. Mulder, "Objective inceptor cueing test for control loading systems: Principle and initial design," in *AIAA Modeling and Simulation Technologies Conference*, 2017, p. 3669.

[14] W. Fu, M. M. Van Paassen, D. A. Abbink, and M. Mulder, "Framework for human haptic perception with delayed force feedback," *IEEE Trans. Human-Machine Systems*, under review.

[15] F. A. A. Kingdom and N. Prins, *Psychophysics: a Practical Introduction*. Academic Press, 2016.

[16] K. Van der El, D. M. Pool, H. J. Damveld, M. M. Van Paassen, and M. Mulder, "An empirical human controller model for preview tracking tasks," *IEEE Trans. Cybernetics*, vol. 46, no. 11, pp. 2609–2621, 2016.

[17] X. D. Pang, H. Z. Tan, and N. I. Durlach, "Manual discrimination of force using active finger motion," *Perception & Psychophysics*, vol. 49, no. 6, pp. 531–540, 1991.

[18] R. J. Adams and B. Hannaford, "Control law design for haptic interfaces to virtual reality," *IEEE Trans. Control Systems Technology*, vol. 10, no. 1, pp. 3–13, 2002.

[19] P. Arcara and C. Melchiorri, "Control schemes for teleoperation with time delay: A comparative study," *Robotics and Autonomous systems*, vol. 38, no. 1, pp. 49–64, 2002.